J. Fluid Mech. (1981), *vol.* 103, *pp.* 117–131
Printed in Great Britain

Experiments on the stability of viscous flow between two concentric rotating spheres

By MANFRED WIMMER
Institut für Strömungslehre und Strömungsmaschinen, Universität Karlsruhe, Germany

(Received 6 September 1978 and in revised form 23 April 1980)

Experimental results concerning the onset of instability in a spherical gap are presented, for the case in which the gap width is not too large with respect to the radius. The two spheres may be rotated in the same direction or in opposite directions. The resulting flow field and some special observations are described. The first onset of instability is recorded and the results are summarized in stability diagrams. It is shown that Taylor's calculations for rotating cylinders are also valid for rotating spheres. Finally, further experimental results by several authors concerning the onset of instability between rotating cylinders are compared with those for rotating spheres.

1. Introduction

In recent years, several papers have been published dealing with experiments of flow between rotating spherical surfaces. All these contributions, for instance Khlebutin (1968), Sawatzki & Zierep (1970), Munson & Meguturk (1975), and Wimmer (1976) are, however, limited to the case of a rotating inner sphere and a stationary outer one. In the case of two spheres rotating independently from each other, greater experimental difficulties arise. This may be the reason why no observations for this case are available, except for some reported in a recent Russian publication by Yavorskaya, Belyaev & Monachov (1977).

The present paper deals with the rotation of both spheres, and it is part of an extensive study of the flow within, between and around rotating spheres (Wimmer 1974). Likewise, this work may be considered as a logical extension of a previous publication by the author (1976) which included preliminary results. Testing methods, fluid, flow visualization, geometry, and the Reynolds-number regime used are similar to those described previously (Wimmer 1976). The test arrangement, however, had to be modified to a certain extent to meet the special conditions to be described here. A second motor was installed which permitted the outer sphere to be rotated independently of the inner one in both clockwise and counter-clockwise directions. Some additional measuring devices to collect data, such as fluid temperature in the rotating system were added.

The problem considered here is closely related to the flow between rotating coaxial cylinders first studied by Taylor (1923) theoretically and experimentally. In succeeding years this type of flow has been subjected to both experimental and theoretical investigations by many authors. Therefore it is of interest to compare the previous results for rotating cylinders with those of rotating concentric spheres to check on their validity for the different geometry.

0022–1120/81/4608–3340 $02.00

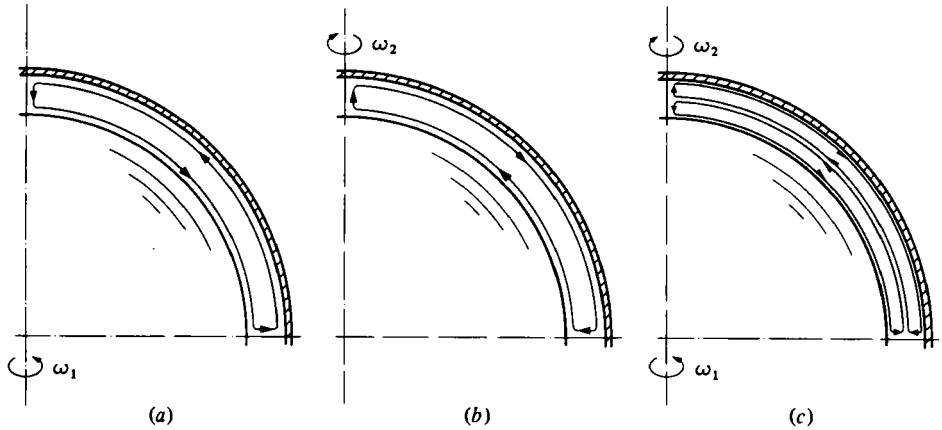

FIGURE 1. Secondary flows. (*a*) Counter-clockwise current for a stationary outer sphere $\omega_2 = 0$; (*b*) clockwise current for a stationary inner sphere $\omega_1 = 0$; (*c*) counter-rotating currents when both spheres rotate in opposite directions.

2. Flow field

The flow field between rotating spheres is different from that between rotating cylinders. In the latter case the basic flow is a circular Couette flow whereas the basic flow between rotating spheres is fully three-dimensional. The flow between two rotating spheres, especially in the vicinity of the inner sphere, is similar to that described in the previously cited references. It depends on the radius ratio and the angular velocity.

The resulting secondary flow, i.e. the flow in a meridional plane between the equator and the poles, is driven by the imbalance of the centrifugal forces within the spherical annulus. The sense of rotation of this swirl is wholly dependent on whether the inner or the outer sphere rotates. For a rotating inner sphere (figure 1*a*) the fluid moves close to the inner sphere from the poles to the equator. In the vicinity of the outer sphere it returns to the poles, so that a counter-clockwise current occurs in the upper right part of the spherical gap. Whereas an outer rotating sphere causes a clockwise current which is independent of the sense of rotation of the sphere as shown in figure 1*b*.

Rotation of the inner sphere generates a potentially unstable layer in contrast to the stable layer produced by the rotation of the outer sphere. As seen in figure 1*c*, these different layers are in contact with each other within the gap. The spheres' angular velocity ratio determines the thickness of the resulting layers which in turn influence the flow field produced. When the spheres are rotated in opposite directions two counter-rotating currents may occur. Furthermore, a nodal radius is generated within the gap at which the angular velocity ω and consequently the circumferential velocity v is zero. The local position of the nodal radius is solely dependent on the angular velocities ω_1 and ω_2. Steady rotation of the spheres in the same direction, with the same angular velocity ($\omega_1 = \omega_2$), results in the exceptional situation of rigid body rotation that includes the fluid.

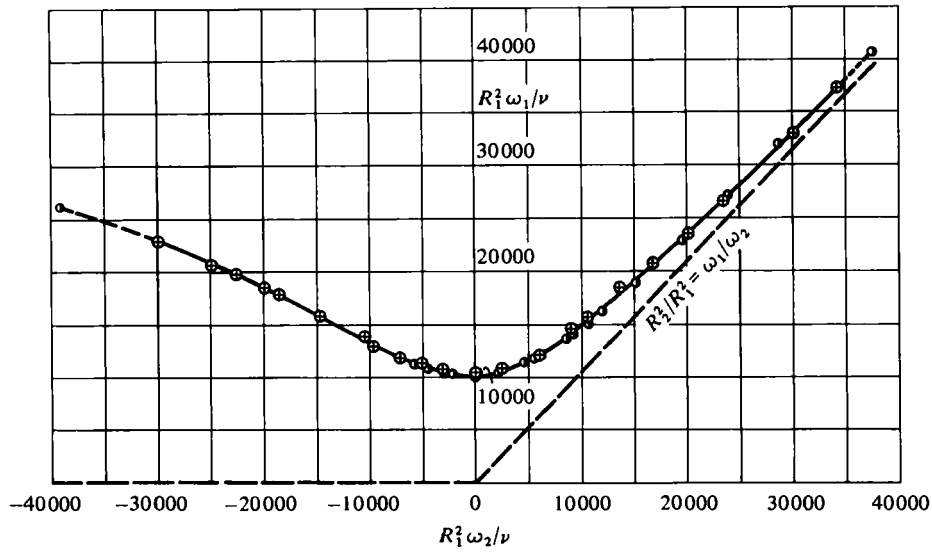

FIGURE 2. Stability diagram for two rotating spheres; $R_1/R_2 = 0{\cdot}975$, $\sigma = 0{\cdot}0256$. ⊕, measurements for concentric spheres; ◑, Taylor's theory for coaxial cylinders.

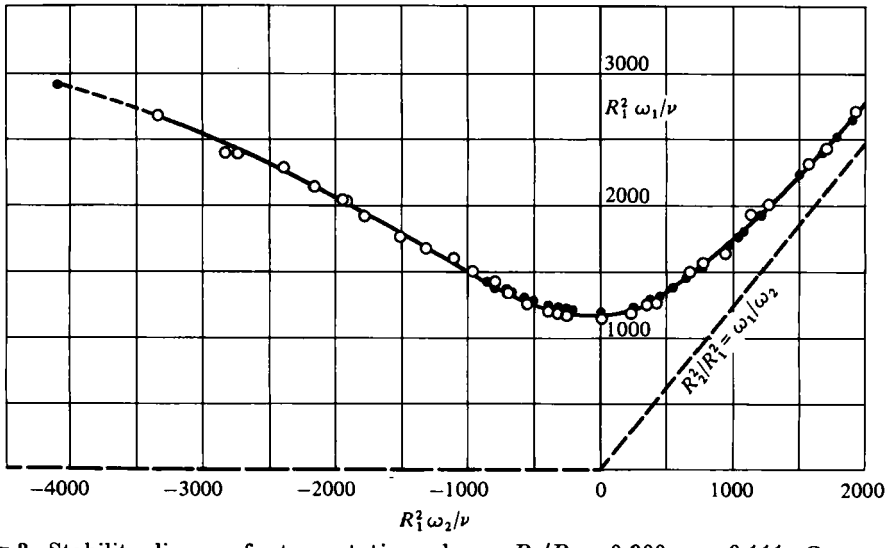

FIGURE 3. Stability diagram for two rotating spheres; $R_1/R_2 = 0{\cdot}900$, $\sigma = 0{\cdot}111$. ○, measurements for concentric spheres; ●, Taylor's theory for coaxial cylinders.

3. Stability diagrams

3.1. *Measurements*

The inner and the outer spheres have radii R_1 and R_2 respectively, and can rotate in the same direction as well as in opposite directions. In both cases instabilities may arise with growing Reynolds numbers. The first onset of instability, seen by eye, was recorded for both cases and varying width of the gap. The results of these experiments are illustrated in stability graphs. Figures 2 and 3 are representative for a relatively

Method	Author	Ta_c Case (*a*)	Ta_c Case (*b*)
Theory for cylinders	Taylor	41·71	43·81
Theory for cylinders	Kirchgässner	41·40	43·63
Theory for spheres	Walton	42·80	43·03
Experiment	Yavorskaya *et al.*	—	44·82
Experiment	Wimmer	41·97	42·99

TABLE 1. Critical Taylor numbers for two sets of spheres. Case (*a*): $R_1 = 7{\cdot}8$ cm, $R_2 = 8{\cdot}0$ cm, $s = 0{\cdot}20$ cm, $\sigma = 0{\cdot}0256$, $R_1/R_2 = 0{\cdot}975$. Case (*b*): $R_1 = 7{\cdot}2$ cm, $R_2 = 8{\cdot}0$ cm, $s = 0{\cdot}80$ cm, $\sigma = 0{\cdot}111$, $R_1/R_2 = 0{\cdot}900$.

small ($\sigma < 0{\cdot}1$) and a relatively large ($\sigma > 0{\cdot}1$) width of the gap ($\sigma = s/R_1$, s = gap width $= R_2 - R_1$). The Reynolds number $Re = R_1^2\omega_1/\nu$ based on the angular velocity of the inner sphere ω_1 is plotted on the ordinate. The corresponding values $R_1^2\omega_2/\nu$ for the outer sphere are plotted on the abscissa (where ω_2 is now the angular velocity of the outer sphere). In the right quadrant, both spheres rotate in the same direction, and in the left quadrant, the spheres rotate in opposite directions. Because the angular velocity of the inner sphere is defined to be positive, the right-hand part of the abscissa is denoted by $+R_1^2\omega_2/\nu$ and the left-hand part by $-R_1^2\omega_2/\nu$ in the following.

The left-hand part of the abscissa and the dashed line in the right quadrant represent a theoretical boundary for stability. This dashed line is valid for inviscid flow and it is based on Rayleigh's (1916) stability criterion $d(\omega r^2)^2/dr > 0$. By dropping all positive terms this expression may be written in the form

$$\omega(\omega_2 r_2^2 - \omega_1 r_1^2) > 0. \tag{1}$$

When both spheres rotate in the same direction, (1) predicts that the product $\omega_2 r_2^2$ must always be greater than $\omega_1 r_1^2$ to obtain stability. With the radius ratio denoted by $\eta(\eta = R_2/R_1 > 1)$, equation (1) requires $\eta^2\omega_2 > \omega_1$. Thus, the angular velocity of the outer sphere ω_2 must be greater than the angular velocity of the inner sphere ω_1 by at least η^2 for stable flow to occur in the gap. Otherwise the motion is unstable. For the gap width $\sigma = 0{\cdot}0256$ and $\sigma = 0{\cdot}111$, these values are 1·05 and 1·23, respectively. If the spheres are rotated in opposite directions, ω changes its sign within the space between the spheres. Therefore (1) is not satisfied within the entire volume of the fluid, i.e. the motion becomes unstable.

Experiments with a viscous fluid in the gap between two concentric rotating spheres show the same behaviour. The width of the gap acts as a geometric parameter. These results are in agreement with those of Yavorskaya, Belyaev & Monachov (1977), who studied the same gap width of $\sigma = 0{\cdot}11$. The noted difference of 4 % for this gap width is within the accuracy of the measurements. It turns out that the critical Reynolds number for $\omega_2 = 0$ given by Yavorskaya *et al.* is about 2 % above and that one of the present experiment gives a value of 2 % below the theoretical value. Table 1 compares critical Taylor numbers for $\omega_2 = 0$ found by different theoretical methods and experiments for the two described gap widths.

An increase in the gap width causes decreasing values of $R_1^2\omega/\nu$. For the two examples described the values differ by one order of magnitude. A contribution by Coles (1967) demonstrates that for rotating cylinders this geometric parameter can be nearly

suppressed by a proper choice of variables when the cylinder's relative sense of rotation is treated separately. As is shown in § 4, these considerations are equally valid for rotating spheres.

Figures 2 and 3 show that the measured values for viscous fluids asymptotically approach the dashed line of Rayleigh's criterion for inviscid flow with increasing values of $+R_1^2\omega_2/\nu$ if the spheres (or cylinders) rotate in the same direction. In the left quadrant, applicable to spheres (or cylinders) rotating in opposite directions, no asymptotic behaviour is detectable. However, an inflexion point occurs so that values of $-R_1^2\omega_2/\nu$ are produced which are higher than $R_1^2\omega_1/\nu$. The consequence is that at constant kinematic viscosity the outer sphere rotates faster than the inner one and nevertheless instability is produced. The motion is unstable, however, only in that region for which Rayleigh's criterion predicts instability. That region covers the portion of the fluid located between the inner sphere and the nodal radius. Beyond the point of inflexion, the nodal radius at which ω and v are zero is shifted in the direction of the inner sphere. Hence, the stable layer of fluid generated by a rotating outer sphere becomes thicker than the unstable layer around the inner sphere. We will call the layer's thickness $\tilde{s}$ and we have $\tilde{s}_{\text{stable}} > \tilde{s}_{\text{unstable}}$. The thickness of the layer producing unstable flow is also smaller than the geometrical gap width so that $\tilde{s}_{\text{unstable}} < s_{\text{geometric}}$. That is why only vortices of shorter wavelength and disturbed flow modes (Wimmer 1976) can be obtained, as they appear for smaller widths of the gap.

The point where the curves intersect the ordinate of figures 2 and 3, designates the onset of instability in the case of a rotating inner sphere and a stationary outer one ($\omega_2 = 0$). The curves fitted to the measured points thereby constitute border lines for real fluids, i.e. below these curves no instabilities in form of Taylor–Görtler vortices are possible and above them the flow is always unstable. The stability boundaries measured for two concentric spheres demonstrate the same behaviour as those calculated by Taylor – and verified experimentally – for two coaxial cylinders.

3.2. *Calculations*

For sufficiently small gap widths, the situation in the immediate vicinity of the equator of the spheres is very similar to that between two cylinders. Furthermore, it is well known that the instabilities always develop in the equatorial plane. Recently Walton (1978) displayed the same facts. In his work the problem of instability of the flow in a narrow spherical annulus is discussed theoretically. Walton deduces that the critical value of the Taylor number T, for which instabilities near the equator first occur, is given by a small correction to the minimum Taylor number for rotating cylinders. Near the equator, this correction is of order σ. He writes

$$T = T_0 + \epsilon T_1, \tag{2}$$

(Walton 1978, p. 690) with $\epsilon \equiv \sigma$ and $T_0 =$ the minimum value 1694·95. The correction term T_1 can be calculated from

$$T_1 = 10^4[(m - \tfrac{3}{4})\pi - 8{\cdot}267/\epsilon - 6{\cdot}78]/8{\cdot}58 \tag{3}$$

where m is an integer which must be calculated separately. Walton (1978) found good agreement between his calculated values and my experimental data (Wimmer 1976).

$R_1 = 7{\cdot}8$ cm, $R_2 = 8{\cdot}0$ cm, $s = 0{\cdot}20$ cm,
$\sigma = 0{\cdot}0256$, $R_1/R_2 = 0{\cdot}975$, $\nu \simeq 0{\cdot}1$ cm²/s

	Experiment		Theory	
μ	ω_2/ν cm^{-2}	ω_1/ν cm^{-2}	ω_2/ν cm^{-2}	ω_1/ν cm^{-2}
0·92	565	614	615·75	669·30
0·90	—	—	471·01	523·34
0·88	386	439	392·02	445·48
0·85	330	388	319·83	376·27
0·80	275	343	249·50	311·87
0·74	225	304	198·54	268·30
0·70	—	—	174·22	248·88
0·65	171	262	149·97	230·72
0·63	151	241	141·62	224·79
0·50	—	—	98·89	197·78
0·48	100	208	93·53	194·85
0·40	—	—	74·11	185·28
0·24	43	178	41·62	173·40
0·20	—	—	34·30	171·52
0	0	168	0	166·96
−0·20	—	—	−33·86	169·31
−0·28	−49	177	−48·21	172·17
−0·40	—	—	−71·50	178 75
−0·44	−82	185	−79·91	181·61
−0·50	—	—	−93·28	186·55
−0·61	−118	195	−120·38	197·34
−0·74	−156	211	—	—
−0·76	−172	227	—	—
−0·93	−242	260	—	—

$R_1 = 7{\cdot}2$ cm, $R_2 = 8{\cdot}0$ cm, $s = 0{\cdot}80$ cm,
$\sigma = 0{\cdot}111$, $R_1/R_2 = 0{\cdot}900$, $\nu \simeq 1{\cdot}7$ cm²/s

	Experiment		Theory	
μ	ω_2/ν cm^{-2}	ω_1/ν cm^{-2}	ω_2/ν cm^{-2}	ω_1/ν cm^{-2}
0·80	—	—	119·08	148·85
0·72	—	—	36·61	50·85
0·71	37·4	52·6	34·36	48·39
0·70	32·7	47·0	32·41	46·30
0·68	30·3	44·7	29·14	42·85
0·63	24·4	38·8	23·32	37·02
0·60	—	—	20·77	34·62
0·59	21·8	37·2	20·02	33·94
0·57	18·0	31·7	18·65	32·72
0·50	14·9	30·1	14·76	29·51
0·45	13·1	29·0	12·55	27·90
0·40	—	—	10·66	26·65
0·33	8·0	24·3	8·36	25·33
0·29	6·8	24·2	7·18	24·75
0·20	4·5	23·1	4·75	23·77
0	0	22·4	0	22·82
−0·20	—	—	−4·62	23·12
−0·22	−5·0	22·7	−5·11	23·22
−0·27	−6·1	23·0	−6·35	23·51
−0·32	−7·5	23·5	−7·64	23·89
−0·40	—	—	−9·87	24·67
−0·45	−10·7	24·0	−11·38	25·28
−0·50	—	—	−12·99	25·97
−0·52	−13·5	26·1	−13·66	26·27

−1·05	−303	293	—	—	−0·56	−15·4	27·3	−15·06	26·87
−1·08	−326	302	—	—	−0·60	—	—	−16·47	27·45
−1·15	−371	324	—	—	−0·64	−18·7	29·1	—	—
−1·21	−410	338	—	—	−0·69	−21·5	31·0	—	—
−1·30	−490	376	—	—	−0·79	−25·3	32·2	—	—
−1·576	—	—	−641·81	427·88	−0·84	−29·0	34·0	—	—
					−0·92	−34·3	37·1	—	—
					−0·94	−36·7	39·1	—	—
					−0·97	−38·0	39·3	—	—
					−1·00	−41·5	41·5	—	—
					−1·05	−46·0	44·0	—	—
					−1·15	−52·7	46·0	—	—
					−1·18	−54·5	46·2	—	—
					−1·24	−64·3	51·7	—	—
					−1·403	—	—	−79·00	56·30

TABLE 2. Experimental and theoretical results for two sets of spheres.

For the two gap widths discussed in the present paper, the critical values are calculated with Walton's method and compared with the experiments. Thus, for a gap width $\sigma = 0{\cdot}0256$ the critical value of the Taylor number $Ta = 42{\cdot}80$ ($Ta = R_1 s\omega/\nu(s/R_1)^{\frac{1}{2}} = T^{\frac{1}{2}}$), with $m = 107$ and $T_1 = 5347$, compared with the experimental value of $Ta = 41{\cdot}97$. For the gap width $\sigma = 0{\cdot}111$ these values are $Ta = 43{\cdot}03$ with $m = 27$ and $T_1 = 1409$, compared with the experimental value of $Ta = 42{\cdot}99$. The difference between experiment and theory is less than 2 %. Such a discrepancy is within the accuracy of the measurements.

On the other hand, Kirchgässner's (1961) theory for the calculation of the critical Reynolds numbers for arbitrary gap widths for rotating cylinders is also applicable for rotating spheres (Wimmer 1976). This fact together with the similarities in the shapes of the stability boundaries clearly indicates the applicability of Taylor's stability calculations also to the case of rotating spheres.

The first step to prove this assertion was to calculate the onset of instability for a rotating inner sphere and a stationary outer one. In the diagrams this is the point on the ordinate where $R_1^2\omega_2/\nu$ equals zero. Using Taylor's notation, the angular velocity ratio ω_2/ω_1 is designated by μ, and rotation in the same and opposite direction is indicated by $+\mu$ and $-\mu$ respectively. Thus, for a stationary outer sphere μ must equal zero. For rotation in the same direction and a small rotation in the opposite direction, the original formula which describes the dependence of the angular velocity ratio on a parameter P can be taken directly from Taylor's paper (1923, p. 309, eq. (5·43)) as

$$P = \frac{\pi^4\nu^2(R_1+R_2)}{2\omega_1^2 s^3 R_1^2(1-R_2^2\mu/R_1^2)(1-\mu)}. \tag{4}$$

The inverse of this value was later called the Taylor number $T = \omega_1^2 s^3 R_1/\nu^2$, for an outer wall at rest and with $s \ll R_1$. Here the parameter P is used with the additional term (Taylor 1923, p. 318, eq. (7·11)) because σ is certainly small but not negligible:

$$P = 0{\cdot}0571\left(\frac{1+\mu}{1-\mu} - 0{\cdot}652s/R_1\right) + 0{\cdot}000\,56\left(\frac{1+\mu}{1-\mu} - 0{\cdot}652s/R_1\right)^{-1}. \tag{5}$$

For a higher speed ratio in the opposite direction, however, Taylor's data must first be modified before application to the special conditions pertaining to a spherical geometry. In doing so, one obtains the angular velocity ratio $\mu = -1{\cdot}576$ for $\sigma = 0{\cdot}0256$ and $\mu = -1{\cdot}403$ for $\sigma = 0{\cdot}111$. Hence, in a range of $-0{\cdot}61 < \mu < 0{\cdot}92$ every point can be calculated and additionally $\mu = -1{\cdot}576$ for $\sigma = 0{\cdot}0256$. For $\sigma = 0{\cdot}111$ the calculated points ranges from $\mu = -0{\cdot}60$ to $\mu = 0{\cdot}80$ with the additional value of $\mu = -1{\cdot}403$. Within these limits, Taylor's calculations may be applied to rotating spheres for both relatively small as well as relatively large gap widths.

Comparison of the theoretical results obtained by the described method and experiments shows excellent agreement. The calculated and the experimental values fall on the same curve in the range of the investigation. The detailed data are listed in table 2. An explanation for the good agreement between the values obtained experimentally for concentric spheres and the values obtained by the calculation for cylinders is provided by the fact already mentioned: for small gap widths, the situation

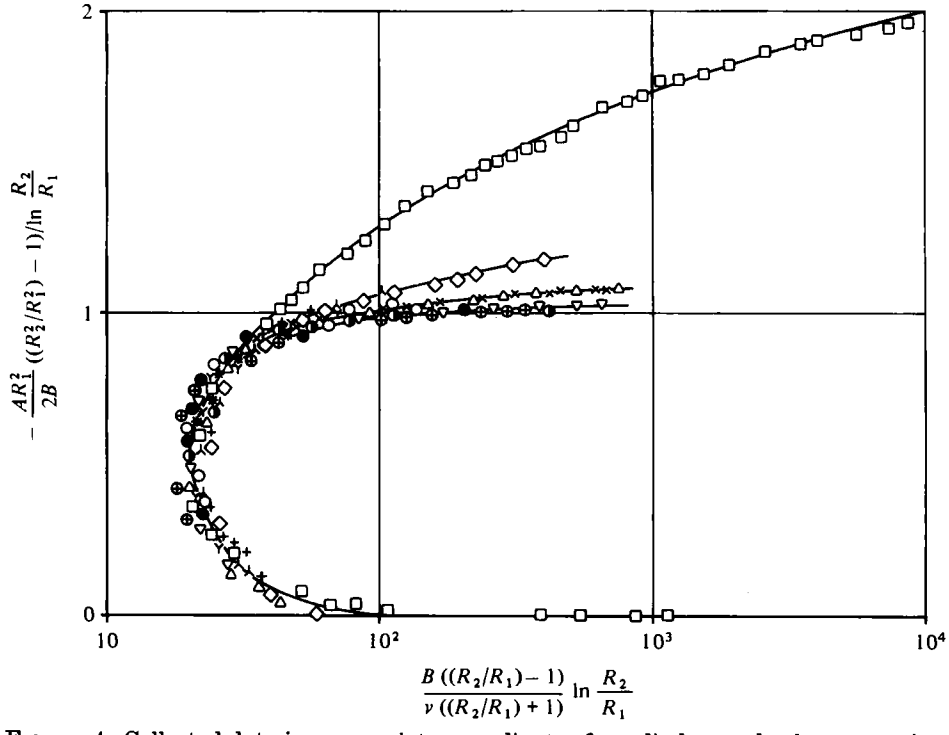

FIGURE 4. Collected data in appropriate co-ordinates for cylinders and spheres rotating in same direction. For coaxial cylinders; R_1/R_2:

□, 0·500, Donnelly & Fultz
+, 0·584, Lewis
⅄, 0·698, Lewis
◇, 0·743, Taylor
Y, 0·736, Lewis
*, 0·854, Lewis
×, 0·873, Coles
△, 0·880, Taylor
▽, 0·942, Taylor

For concentric spheres; R_1/R_2:

○, 0·900, Wimmer, experiment
●, 0·900, Wimmer, theory
⊕, 0·975, Wimmer, experiment
◑, 0·975, Wimmer, theory

in the immediate vicinity of the equator of the spheres, where the Taylor vortices always develop first, is nearly the same as that between rotating cylinders. Thus, we are justified in stating that stability diagrams for the flow between spherical surfaces can be obtained not only from experiments but also from a theoretical method.

4. Comparison with cylinders using Coles' diagrams

As mentioned above, most of the considerations concerning the onset of instability between rotating cylinders are also valid for rotating spheres. In order to prove this statement, the critical data for rotating spheres are here compared with those for rotating cylinders. Coles (1967) nearly suppressed the geometrical parameter by treating rotation in the same direction and in opposite directions as separate cases. Coles collected the data of several authors concerning the onset of instability between

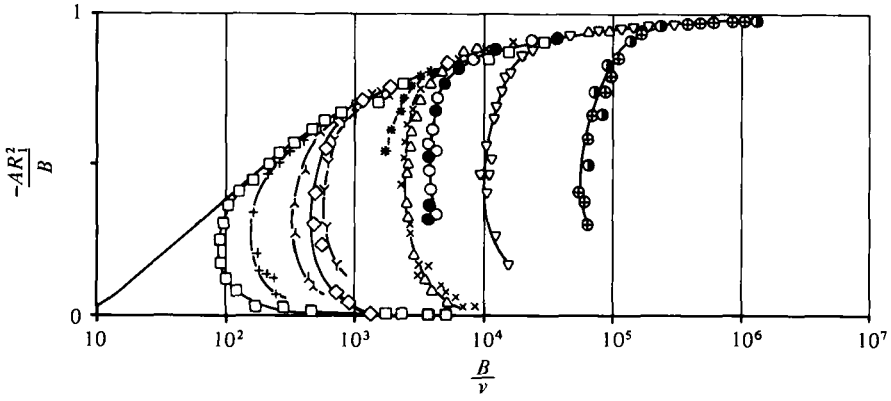

FIGURE 5. Collected data in appropriate co-ordinates for cylinders and spheres rotating in opposite directions. For legend, see figure 4.

rotating cylinders, for a wide range of gap withs, and this data is reproduced here. The new critical data for rotating spheres are represented by circles in the Coles' diagrams as is shown figures 4 and 5.

The co-ordinates and the quantities A and B are based on the formula $v = Ar + B/r$ obtained for a steady Couette flow between rotating cylinders. However, the basic flow in a spherical annulus is described for low Reynolds numbers by

$$v = (Ar + B/r^2)\sin\theta.$$

Thus, the constants A and B are different in the case of spheres. For small spherical gap widths the flow near the equator is, however, very similar to that between rotating cylinders as also noted by Walton (1978). The constants A and B are analogously similar for the spherical gap flow near the equator ($\sin\theta = 1$) in comparison to the cylindrical case. The simpler formula for rotating cylinders was in fact also found to be sufficient for describing the initiation of instability between spherical walls, at least for small and moderate gap widths.

The figures show that the critical data for rotating spheres exhibit the same behaviour as the data for cylinders rotating in both the same and opposite directions. Therefore, the above mentioned assertion is confirmed. For small and moderate gap widths, the flow in the immediate vicinity of the equator of the spheres is similar to that between two coaxial cylinders. Consequently, one can conclude that the first appearance of Taylor vortices, which always develop at the equator, follows the same trends as those established for the cylindrical case. Hence, it is evident that – at least for small and moderate gap widths – stability diagrams for the flow between rotating spheres may be obtained theoretically without engaging in experimentation.

5. Some characteristic flow observations

When both spheres rotate flow phenomena are observed which do not appear when the outer sphere is stationary. Aside from the difference between the wavelength of the vortices and the geometrical gap width for counter-rotating spheres, contours of the developing vortices are produced which are not so sharp as when the outer sphere

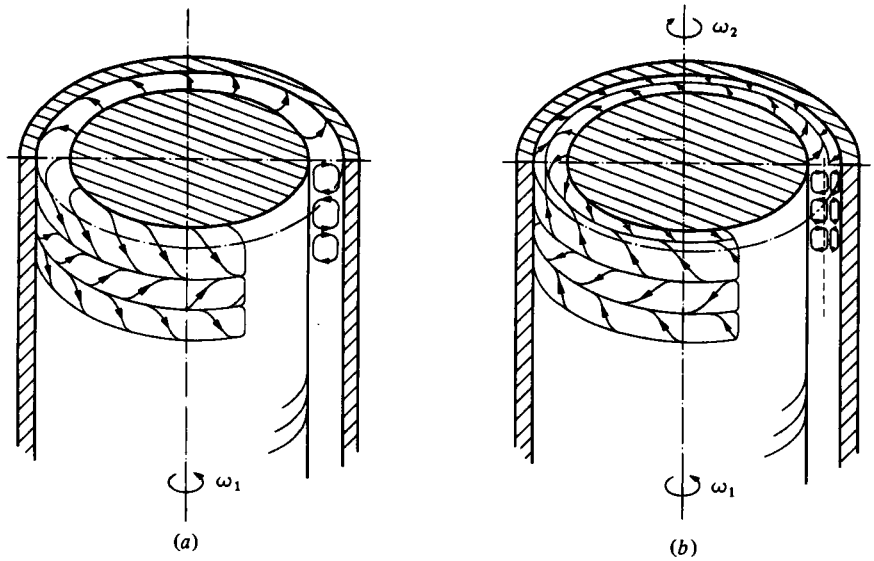

FIGURE 6. Streamlines of the vortices in the cylindrical case. (*a*) Inner cylinder rotates, outer one at rest; (*b*) counter-rotating cylinders.

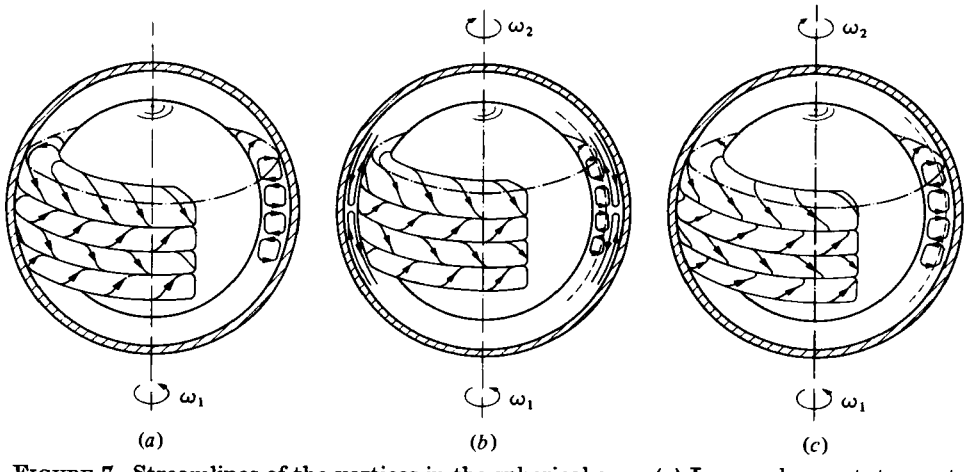

FIGURE 7. Streamlines of the vortices in the spherical case. (*a*) Inner sphere rotates, outer one at rest, (*b*) fast counter-rotating spheres; (*c*) slightly counter-rotating spheres.

is stationary. This behaviour is caused by two effects acting independently of each other. These effects are due to the spherical gap flow and they do not occur for the flow between rotating cylinders. For a rotating inner cylinder and an outer one at rest the well known sharply divided pattern of vortices is apparent, as shown in figure 6*a*. For the case of counter-rotating cylinders, the space between the cylindrical walls is divided into two different parts: an inner part with vigorous vortices that have still nearly square cross-sections and an outer part with deformed vortices having a very much weaker opposite rotation. These vortices – the inner and the outer ones – are in contact with each other, i.e. the outer weaker vortices are induced by the vigorous

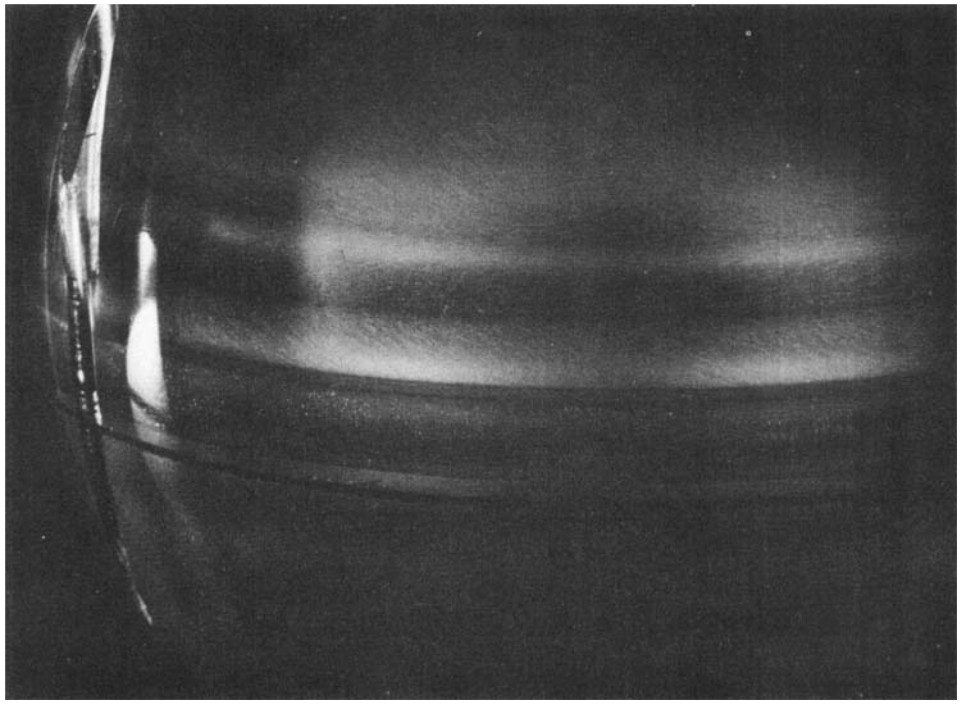

FIGURE 8. Streamlines of the vortices for a rotating inner sphere and outer one at rest; $\mu = 0$.

inner ones (figure 6*b*). That part of the gap width, however, which may be unstable according to the theory (here the square of the circulation decreases with the radius), is larger in the experiment than would be expected by the theory (dashed lines in figures 6*b*, 7*b*, *c*). The outer vortices with very weak rotation exist only since the basic flow in the cylindrical case is purely one-dimensional, i.e. a circular Couette flow. As a consequence we see the same pattern as if the outer cylinder were at rest (figures 6*a*, *b*).

For a rotating inner sphere with the outer one at rest the pattern of the S-shaped streamlines of the vortices can be observed. This pattern is the same as that of the cylindrical case, as shown in figures 7(*a*) and 8. In contrast to the cylindrical case the basic flow between rotating spheres is fully three-dimensional (figure 1*c*). The consequence for a sufficiently large counter-rotation is that the very weak vortices of the outer range, which are on the point of developing, are carried with the basic flow up to the poles, and are not established at all. So a purely undisturbed big meridional loop occurs which acts like an optical filter with respect to the observed vortices. Figure 7(*b*) illustrates that behaviour. The same pattern of the S-shaped streamlines of the vortices appears, although it is less pronounced. For slightly counter-rotating spheres the vigorous vortices linked to the inner wall are again larger than the theoretically expected spacing. Therefore, they extend to the outer spherical shell. Due to the non-slip condition for viscous fluids the portion of the fluid near the outer wall is dragged along in the direction of the outer spherical shell. This results in a deformation of the streamlines of the vortices. As seen in figure 7(*c*) and 9, the streamlines

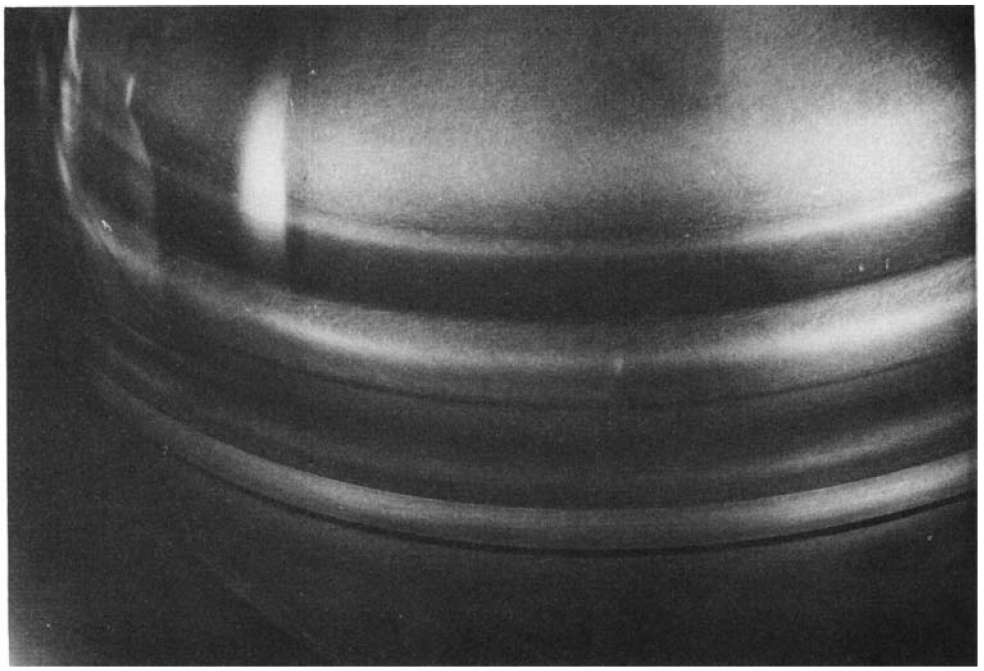

FIGURE 9. Streamlines of the vortices for slightly counter-rotating spheres; $\mu = -0{\cdot}07$.

now become U-shaped. The strength of the deviation is dependent on the speed of the outer sphere. Because of the deviation the light is reflected in another way displaying less contrast with respect to the vortices' shapes.

In the case of counter-rotating spheres, it is very difficult to determine precisely when the transition to unstable flow occurs. The difficulty arises from the high angular velocities involved. Quite often disturbances caused by a spiral instability occur around the pole (Wimmer 1976). For spheres rotating in opposite directions, it is possible to create the spiral instability around the pole earlier than that of the Taylor–Görtler type at the equator. By increasing the angular velocity, the arms of the spirals are extended downward to the equatorial plane and they influence the developing Taylor vortices. These differing types of instability overlap each other and the whole configuration becomes wavy. As a consequence, the first onset of instability is more difficult to detect in this special case, resulting in a decrease in the accuracy of the measurements. We have 5 % accuracy of the critical Reynolds numbers for rapid counter-rotation as compared to about 2 % for all other cases.

6. Conclusions

The behaviour of instabilities which arise in fluids enclosed between two rotating spherical surfaces is, in principle, similar to that for a rotating inner sphere and a stationary outer one. There are, however, some differences. When only the inner sphere rotates, the entire portion of the fluid between the spheres may be unstable according to Rayleigh. Thus, the unstable layer's thickness equals the gap width and is always constant. Another result of a previous paper (Wimmer 1976) shows that the

behaviour of the vortices is completely different for gap widths $\sigma < 0{\cdot}1$ than for $\sigma > 0{\cdot}1$. Rotating the spheres in opposite directions generates different sizes of an unstable layer for different angular velocity ratios. Consequently, the thickness of the unstable layer is always smaller than the geometrical gap width. Hence, vortices are produced with a smaller wavelength. This implies that the disturbed flow modes correspond to those for smaller widths of the gap. Furthermore, the shapes of the vortices display less contrast when both spheres are rotated. This effect is most noticeable when the spheres are counter-rotated. The explanation for this effect was discussed in the previous text.

A comparison of the experimental and theoretical results concerning the instabilities show good agreement. Walton's (1978) theoretically obtained data are within the accuracy of the measurements. The calculations of Taylor (1923) and Kichgässner (1961), as well as Coles' (1967) method of suppressing the geometrical parameter – all derived for rotating cylinders – are applicable to rotating spheres without serious restrictions. Thus, it has been proven that stability diagrams depicting the flow between rotating spheres with small and moderate gap widths can be obtained theoretically without resort to laborious measurements.

Further tasks remaining are to clarify the degree to which the methods described herein are applicable for very wide spherical gap widths. There, as reported by Munson & Menguturk (1975), no regular Taylor vortices are detectable utilizing the method of flow visualization. A possible method may be to determine the critical values employing friction torque measurements and to translate them into stability diagrams. This work will surely require a greater experimental effort. It is assumed, however, that the transition points for larger gap widths can fit into the procedure described above, at least up to those gap widths for which the previously mentioned methods are valid for the cylindrical case itself.

Some of the results described in this paper were reported at the Euromech Colloquium 56 in London in 1975 and at the GAMM-meeting in Graz, Austria, in 1976 (Wimmer 1977).

A referee has pointed out that a similar Rayleigh criterion for spheres has been obtained by A. M. Waked & B. R. Munson. Experiments on the stability of the flow in a spherical annulus are also presented in this work, which was published in the Journal of Fluids Engineering, vol. 100, 1978, after the present paper was first sent to the Journal of Fluid Mechanics.

REFERENCES

Coles, D. 1967 A note on Taylor instability in circular Couette flow. *Trans. A.S.M.E.*E, *J. Appl. Mech.* **34**, 529.

Donnelly, R. J. & Fultz, D. 1960 Experiments on the stability of viscous flow between rotating cylinders. II. Visual observations. *Proc. Roy. Soc.* A **258**, 101.

Khlebutin, G. N. 1968 Stability of fluid motion between a rotating and stationary concentric sphere. *Fluid Dyn.* **3**, 31.

Kirchgässner, K. 1961 Die Stabilität der Strömung zwischen zwei rotierenden Zylindern gegenüber Taylor–Wirbeln für beliebige Spaltweiten. *Z. angew. Math. Phys.* **12**, 41.

Lewis, J. W. 1928 An experimental study of the motion of a viscous liquid contained between two coaxial cylinders. *Proc. Roy. Soc.* A **117**, 388.

MUNSON, B. R. & MENGUTURK, M. 1975 Viscous incompressible flow between concentric rotating spheres. *J. Fluid Mech.* **69**, 705.

RAYLEIGH, LORD 1916 On the dynamics of revolving fluids. *Proc. Roy. Soc.* A **93**, 148.

SAWATZKI, O. & ZIEREP, J. 1970 Das Stromfeld im Spalt zwischen zwei konzentrischen Kugelflächen, von denen die innere rotiert. *Acta Mech.* **9**, 13.

TAYLOR, G. I. 1923 Stability of a viscous liquid contained between two rotating cylinders. *Phil. Trans.* A **223**, 289.

WALTON, I. C. 1978 The linear stability of the flow in a narrow spherical annulus. *J. Fluid Mech.* **86**, 673.

WIMMER, M. 1974 Experimentelle Untersuchungen der Strömung im Spalt zwischen zwei konzentrischen Kugeln, die beide um einen gemeinsamen Durchmesser rotieren. Dissertation, Universität (T.H.) Karlsruhe.

WIMMER, M. 1976 Experiments on a viscous fluid flow between concentric rotating spheres. *J. Fluid Mech.* **78**, 317.

WIMMER, M. 1977 Experimentelle Untersuchung der Strömung zwischen konzentrischen, rotierenden Kugeln. *Z. angew. Math. Mech.* **57**, 218.

YAVORSKAYA, I. M., BELYAEV, YU. N. & MONACHOV, A. A. 1977 Investigation of the stability and secondary flows in rotating spherical fluid layers at arbitrary Rossby numbers (in Russian). *Dokl. Akad. Nauk.* **237** (4), 804.